Dielectric properties of heavily doped crystalline and amorphous silicon from 1.5 to 6.0 eV

D. E. Aspnes,* A. A. Studna,* and E. Kinsbron
AT&T Bell Laboratories, Murray Hill, New Jersey 07974
(Received 12 July 1983)

Extremely uniform, microscopically smooth, large-grained polycrystalline Si films saturation doped with phosphorous to a carrier concentration $n=3.3\times10^{20}$ cm^{-3} were prepared by a combination of low-pressure chemical-vapor-deposition and heat-treating processes to obtain samples suitable for measuring the small effects of large impurity concentrations on the above-band-gap dielectric properties of Si. From 1.5 to 2.5 eV, the effects of heavy doping are described by the Drude free-carrier model with lifetimes determined by scattering from lattice vibrations. Above 3 eV, the dielectric function spectrum of heavily doped Si is remarkably similar to that of undoped material except that the E_1 and E_2 structures are broadened and shifted to lower energies. The impurity-induced broadening is much larger for E_1 than for E_2, indicating that a metastable excitonic resonance is well developed for the former but not for the latter. Present and previous data of the authors, together with previous data of Viña and Cardona, are consistent with an approximately linear shift of the threshold energy with impurity concentration. This indicates that the dominant mechanism responsible for the shifts is the effect of the random impurities on the crystal potential. While the possibility of electron-electron and electron-ion interactions on the electron and hole self-energies cannot be ruled out, comparison with recent calculations of Berggren and Sernelius show that these effects must be much smaller at higher interband transitions than at the fundamental indirect band gap. Using our data as a reference, we show that the anomalous absorption observed by Jellison and co-workers for As-implanted and laser-annealed c-Si is due to microscopically rough surface layers on their samples. Consequently, the differences that they observe between P and As dopants must involve differences in recrystallization and regrowth. Dielectric-function spectra for amorphous Si films doped *in situ* with phosphorus are essentially identical within microstructural effects to those of undoped material, indicating no significant influence from heavy doping. At energies below 3.2 eV, the data expressed as $(\alpha nE)^{1/3}$ or as $(\epsilon_2)^{1/2}$ both vary nearly linearly with energy, suggesting nondirect transitions between simple parabolic bands with momentum matrix elements linearly proportional to E or with dipole elements independent of E.

I. INTRODUCTION AND SUMMARY

The increase of absorption and the appearance of structure due to plasma resonances in the optical spectra of semiconductors in the infrared are two consequences of heavy doping that are well understood.[1,2] In contrast, much less is known about the effects of large densities of free carriers and ionized impurities on energy band thresholds and the dielectric properties of semiconductors at and above the fundamental absorption edge. The subject has received much recent experimental and theoretical attention both as a model many-body system and as a necessary aspect of submicron-device technology. Experimental work at the fundamental indirect gap of Si has been summarized by Keyes,[3] and the theoretical understanding of the heavy doping problem has been discussed by Berggren and Sernelius[4] and by Selloni and Pantelides.[5]

Accurate data describing the effects of heavy doping on the dielectric response and band structure of semiconductors above the fundamental absorption edge are limited. Here, large densities, of the order of 0.1—1 at. % or more, are necessary to produce observable effects.[6] These impurity concentrations have traditionally been obtained by bulk doping or by ion implantation followed by laser annealing. But heavily doped bulk samples are difficult to polish,[6] and as we shall demonstrate, the dielectric response data for ion-implanted and laser-annealed material recently reported by several groups[7,8] show unmistakable evidence of microscopic roughness. Microscopic roughness, whether due to polishing or recrystallization, causes pseudo- (perceived or apparent) optical or dielectric functions measured by reflectance or reflectance-polarimetric techniques to differ from their true bulk values. While these differences have only a minor effect on critical-point threshold energies deduced from these spectra, the effect on amplitudes and line shapes can be pronounced.[9,10] More seriously, if these effects are not taken into account, incorrect conclusions about the physics of heavy doping can be drawn. The proper treatment of microstructural artifacts is particularly important when effects on the scale of perturbations are being investigated.

In this work we report accurate dielectric function spectra $\epsilon=\epsilon_1+i\epsilon_2$ obtained from large-grain polycrystalline Si (p-Si) films prepared from dense, extremely flat amorphous Si (a-Si) films deposited by recently developed low-pressure chemical-vapor-deposition (LPCVD) techniques.[11] These a-Si films were simultaneously crystallized and saturation doped with phosphorus by heat treating in a PBr_3 atmosphere. This procedure is known to produce exceedingly uniformly doped films that retain their original surface flatness.[12,13] In addition, we developed a novel self-consistent transmission-reflection

ellipsometric procedure to explicitly determine the parameters of the microscopically rough region and to correct the ϵ data over the 1.5- to 6.0-eV spectral range for its presence. Using these sample and measurement techniques, we have been able to eliminate microstructural artifacts and thus to determine unambiguously the effects of heavy doping on the dielectric properties of Si. Similar procedures were used to obtain the optical properties of a-Si, except that the films were doped *in situ*.[11,14]

The optical results for heavily doped p-Si are shown in Fig. 1, which compares our previously measured ϵ spectrum[15] for lightly doped ($n=2.1\times10^{14}$ cm^{-3}) single-crystal silicon (c-Si) with that obtained here for the saturation-doped polycrystalline material. As anticipated, the intrinsic effect of heavy doping on the above band-gap dielectric response is indeed small and consequently difficult to measure accurately. For example, even on this specially prepared sample the microscopically rough surface region accounts before correction for about $\frac{1}{3}$ of the observed difference between ϵ_2 spectra at the E_2 peak in ϵ_2 near 4.3 eV.

In the semitransparent region below 2.7 eV, free-carrier effects appear mainly in ϵ_1. We show that they are accurately described by the Drude theory, which yields the mean lifetime and volume density of free carriers. The lifetime at room temperature is found to be consistent with that calculated for phonon scattering.[1] The optically determined free-carrier density of $n=3.3\times10^{20}$ cm^{-3} is exactly equal to that[16,17] determined by transport measurements on similar saturation-doped films. Another consistency check is obtained by comparing our spectroscopic ellipsometric results for undoped and heavily doped material. We find that systematic errors cannot exceed $\sim0.02\%$ for either set of data.

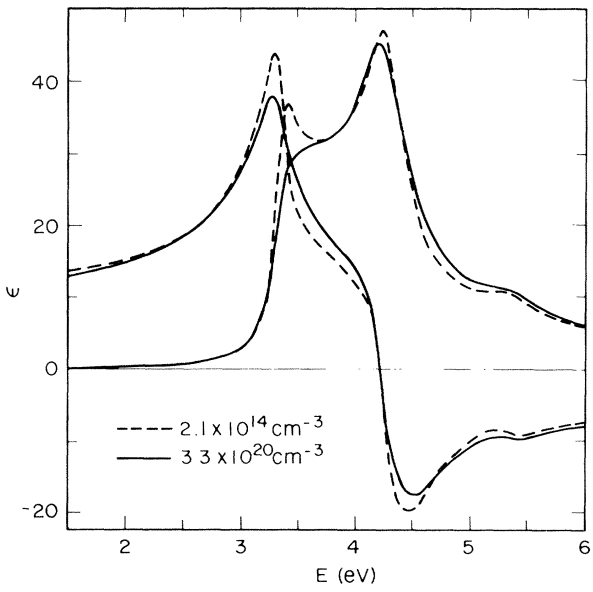

FIG. 1. Dielectric response ϵ of a P-doped large-grain polysilicon film with $n=3.3\times10^{20}$ cm^{-3}. Pseudodielectric function $\langle\epsilon\rangle$ from Ref. 15 of a lightly doped ($n=2.1\times10^{14}$ cm^{-3}) silicon crystal is also shown for comparison.

Above 3 eV, the major effects of heavy doping are a broadening of the E_1 and E_2 structures and a shift of the corresponding critical-point thresholds at 3.4 and 4.3 eV, respectively, to lower energy. The Thomas-Fermi screening length $L_{TF}\cong5$ Å is much less than the calculated radii of possible metastable excitonic resonances associated with these transitions, which shows that these resonances would be screened by the large density of free carriers. The fact that only E_1 is broadened appreciably shows that a significant excitonic resonance can exist only at this threshold. The overall similarity between the ϵ spectra of lightly and heavily doped material at other energies shows that the free-carrier screening has negligible influence at general points in the Brillouin zone.[18]

The shifts of the critical-point thresholds to lower energy in our present data, our previous results on As-implanted and laser-annealed material,[7] and recent spectroscopic ellipsometric (SE) measurements of Viña and Cardona[19] are compared to the many-body calculations of Berggren and Sernelius[4] and to the Boltzmann formalism of Allen and co-workers.[20–22] The dependence on impurity concentration when all data are considered is approximately linear, indicating that the predominant effect of heavy doping on these thresholds is not exchange or correlation but the influence of the randomly substituted impurity potentials on the unperturbed lattice. The effect can be qualitatively described as a second-order correction of the energy levels of the unperturbed crystal.[20] Electron-electron and screened electron-ion contributions to the electron and hole self-energies can be eliminated as major effects because the expected threshold dependences of $n^{1/3}$ and $n^{1/2}$, respectively,[4] are not apparent from the data. At the very least, the self-energy shifts must be significantly less than those calculated[4] for the fundamental indirect edge. Because the formal expressions for these self-energies are $\vec{k}$ dependent, there is of course no reason to assume that the fundamental-edge values should be valid everywhere in the zone. A specific calculation is needed.

By providing accurate reference spectra, our results allow microstructural effects in previously reported data to be identified. Our earlier data on comparably doped As-implanted and laser-annealed samples[7] show no measurable difference in the bulk dielectric response but show that the samples were covered with a microscopically rough surface layer 16 Å thick. We also find that the "anomalous" absorption reported in spectroscopic ellipsometric measurements of similar As-implanted and laser-annealed sample by Jellison and co-workers[8] can be entirely explained by a similar microscopically rough surface region on their samples. Because Jellison *et al.* did not observe such surface regions on P-implanted samples,[8] we can conclude from our analysis that the As-P differences do not pertain to bulk doping but rather to differences in the recrystallization and regrowth mechanisms for the different types of implanted atoms.

For completeness, ϵ spectra were also obtained on a-Si films doped *in situ* with phosphorus. However, microstructural effects seemed to outweigh the effects of heavy doping, and no effects obviously related to a large free-carrier concentrations could be seen. Our results agree

well with our previous data on LPCVD films[23] and with those of Drevillon *et al.*[24] on magnetron-sputtered material, indicating a now quite general convergence on an "intrinsic" dielectric response for a-Si. Our more accurate data for ϵ_2 allowed us to investigate the functional dependences of various powers of α and ϵ_2 on energy. We found that the standard Tauc functional dependence[25] $(\epsilon_2 E)^{1/2}$ predicted to be linear in E for nondirect transitions between simple parabolic bands for a constant-momentum matrix element shows, in fact, considerable curvature. In contrast, the functional forms $(\alpha n E)^{1/3}$ and $(\epsilon_2)^{1/2}$ were each quite linear in energy and no distinction could be made between them to within experimental accuracy. The former variation was predicted by Davis and Mott[26] for nondirect transitions between simple parabolic bands where the momentum matrix element varies linearly with energy, while the latter variation was predicted by Cody *et al.*[27] for a similar situation but where the *dipole* matrix element is constant. Our results are therefore consistent with recent results of Klazes *et al.*[28] on sputter- and glow-discharge-deposited a-Si films.

II. EXPERIMENTAL

The starting material for the large-grained p-Si films were extremely dense, smooth a-Si films nominally 5000 Å thick deposited at 591 °C by LPCVD on thermally oxidized c-Si wafers. The deposition procedure is described elsewhere.[11] The samples were converted to large-grained polycrystalline material and simultaneously saturation doped with P by heating in a PBr_3 atmosphere at 1000 °C for 30 min. The attractive feature of this procedure is that the p-Si film retains the original flatness and density of the original a-Si film.[12,13] Because uniformity was critical for unambiguously determining the small free-carrier effects on ϵ, we did not attempt to prepare samples of varying carrier concentrations but restricted our experimental investigations strictly to saturation-doped material.

In order to assess independently the uniformity in thickness and grain size of the films and to obtain their thicknesses relative to that of the nominally 1000-Å-thick thermal oxide, the samples were fractured after optical measurement and transmission electron micrographs were made of thinned sections of the films. The micrograph of the p-Si sample used to obtain the data of Fig. 1 is shown in Fig. 2. The scale is set by the 1000-Å thickness of the thermal oxide. The film is clearly polycrystalline, with grain sizes ranging from 500 to 2000 Å, and the surfaces and interfaces are sharp on the resolution scale of the instrument. Figure 2 shows that the thickness ratio d_2/d_1 of the p-Si film and the thermal oxide is 5.29 ± 0.05. Independent optical measurements of a part of the sample stripped of the p-Si film showed that $d_1 = 1002\pm2$ Å, whence $d_2 = 5300\pm50$ Å providing an independent check of the data-reduction procedure.

The heavily doped a-Si films were prepared by *in situ* doping with PH_3 during LPCVD deposition at 571 °C.[11,14] TEM (transmission electron microscopy) micrographs showed these films to be nearly completely amorphous. Electrical measurements[12] on similar films show carrier concentrations of the order of $n \cong 4\times10^{20}$ cm^{-3}. Optical properties from 1.5 to 6.0 eV were determined by spectroscopic ellipsometry. To minimize overlayer effects and to ensure a negligible contribution from natural oxides, all

FIG. 2. Micrograph of the cross section of the heavily doped large-grain polycrystalline film used to obtain the data of Fig. 1. The 1000-Å thermal oxide and single-crystal Si substrate are the dark and light gray regions, respectively.

samples were optically aligned in the ellipsometer, rinsed successively with methanol, water, and 10 vol% HF in methanol, and maintained in a dry N_2 atmosphere as described previously.[29] The rotating-analyzer ellipsometer used to obtain the complex reflectance [$\tan\psi$, $\cos\Delta$ (TC)] and pseudodielectric function ($\langle\epsilon\rangle$) spectra and methods of compensating for the optical activity of the quartz Rochon prisms have also been discussed elsewhere.[30,31]

III. DATA AND ANALYSIS

The necessity of determining and then eliminating microstructural effects requires a different method of analysis from those previously used for the interpretation of ellipsometric spectra. Consequently, we outline our approach in this section. Below a certain energy, the a- and p-Si films are weakly absorbing, and strong interference oscillations are obtained. These can be seen clearly in Fig. 3, which shows the complex reflectance spectrum $\rho=(\tan\psi)\exp(i\Delta)$ calculated from the TC data for the p-Si sample shown in Fig. 2. At sufficiently high energies the films become opaque and pseudodielectric function data $\langle\epsilon\rangle=\langle\epsilon_1\rangle+i\langle\epsilon_2\rangle$ can be measured directly. These $\langle\epsilon\rangle$ data are only approximations to the true bulk response ϵ and must be corrected for overlayers such as microscopic roughness. We shall show that the key to correcting the $\langle\epsilon\rangle$ data lies in the analysis of the ρ spectra in the interference-oscillation regime.

The TC data themselves do not determine ρ uniquely when interference is present, but leave a sign ambiguity in Imρ due to the sign ambiguity in the calculation of $\sin\Delta$ as $\pm(1-\cos^2\Delta)^{1/2}$. We eliminate this ambiguity in a novel but simple way by calculating the Kramers-Kronig transformation of Reρ, then comparing the result to the calculated Imρ spectrum. For example, this procedure shows immediately that Imρ in Fig. 3 is positive for exactly three data points near 2.9 eV, that is, just before Imρ drops completely below the real axis. This result would be extremely difficult to deduce from the original pattern, and in fact, was not detected (and a resulting data reduction artifact not eliminated) until the Kramers-Kronig approach was developed.

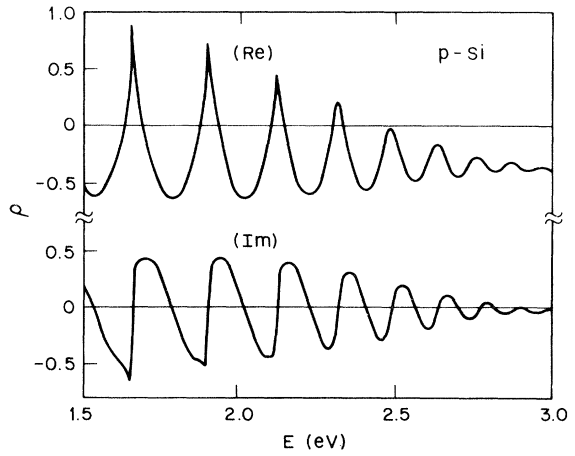

FIG. 3. Complex reflectance ratio of the sample of Fig. 2 in the spectral range where the p-Si film is semitransparent.

Figure 2 shows that the analysis of data in the interference regime requires a model consisting of at least four distinct regions—the c-Si substrate, the thermal oxide, the Si film, and the ambient. To this must be added a boundary region between the film and the ambient because microscopic roughness produces a dielectric response that is distinctly different from that of either adjacent phase. In principle, similar transition regions should also be included at the two interfaces of the thermal oxide. However, the contrast between the dielectric properties of either oxide-semiconductor interface and the oxide itself is much lower, and the neglect of the interface regions at these boundaries will result mainly in a renormalization of the oxide thickness to slightly larger values. The computed dielectric response of the Si film will not be affected.

Consequently, we are led to a five-phase representation consisting of the c-Si substrate, the thermal oxide of thickness d_1, the Si film of thickness d_2, the microscopically rough surface region of thickness d_3, and the dry N_2 ambient. The dielectric response of the c-Si substrate ϵ_s is known from previous measurements[15] while that of the first layer ϵ_{l1}, can be calculated from Malitson's dispersion equation for fused silica.[32] Other known quantities are the angle of incidence ϕ, the dielectric response $\epsilon_a=1$ of the ambient, and the complex reflectance ratio ρ at each measurement energy E. The unknown parameters are the three thicknesses d_1, d_2, and d_3, the void fraction f_v describing the microscopic roughness, and the dielectric function ϵ_{l2} of the Si film. Of the unknowns, only ϵ_{l2} is energy dependent, while the rest are constant over the spectrum. We may therefore write

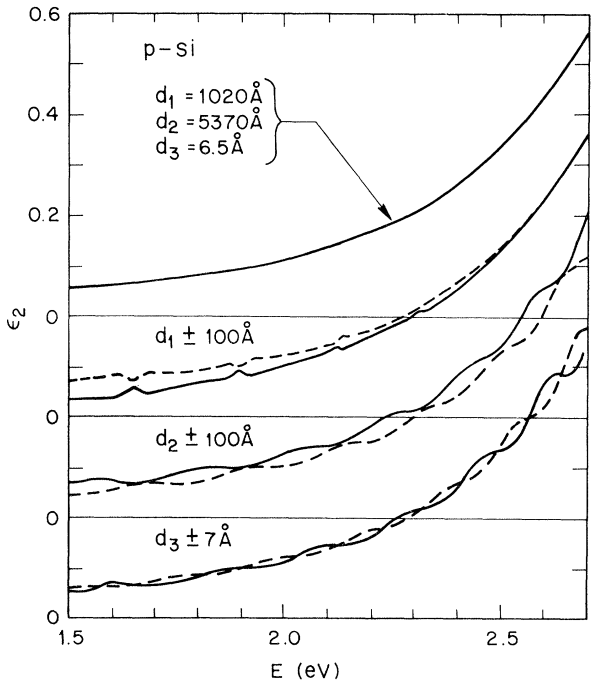

FIG. 4. Exact solution for the imaginary part of the dielectric function of the p-Si film of Fig. 2 obtained by solving Eq. (1) with $f_v=0.6$ and the other energy-independent parameters as indicated (top). Artifacts induced by increasing (dashed lines) or decreasing (solid lines) the individual layer thicknesses by the amounts given (bottom).

$$\rho=\rho(\epsilon_s;\epsilon_{I1},d_1;\epsilon_{I2},d_2;f_v,d_3;E,\phi)\ , \tag{1}$$

which is a schematic representation of the Fresnel reflection equations for a multilayer stack,[33] with the dielectric function of the last layer calculated in the Bruggeman effective-medium approximation (EMA).[34] Equation (1) must be solved for d_1, d_2, d_3, f_v, and ϵ_{I2} from the available data.

To solve Eq. (1), we adopt the strategy of choosing initial values for all energy-independent parameters and then determine ϵ_{I2} at each E. Since Si has no transition thresholds from 1.5 to 3.0 eV, the physically correct solution will correspond to those values of d_1, d_2, d_3, and f_v for which ϵ_{I2} is featureless and simply varies smoothly into the lower pseudodielectric function range of the film.

The solution for $\mathrm{Im}\epsilon_{I2}$ according to these standards is shown from 1.5 to 2.7 eV in an expanded vertical scale at the top of Fig. 4. It is seen that the solution obtained for $d_1=1020$ Å, $d_2=5370$ Å, $d_3=6.5$ Å, and $f_v=0.6$ is mathematically smooth on this scale. To assess the sensitivity to these parameters, we show on the same scale but with different origins the corresponding solutions that result from increases (dashed lines) or decreases (solid lines) of the three thicknesses by 100, 100, and 7 Å, respectively. An error in any d_i generates a unique interference-related artifact in the ϵ spectrum itself. Changes in d_1 for the thermal oxide show a resonance-type behavior and are more pronounced at long wavelengths where the p-Si film is more transparent. Conversely, the effect of roughness (d_3) is largest at higher energies. An error in d_2 generates oscillations of a different phase than those of d_3 and the amplitude is uniform over the whole range.

From these results we estimate our uncertainties in d_1, d_2, and d_3 for this sample to be ±25, ±25, and ±1 Å, respectively. The values of d_3 and f_v interact so the latter uncertainty is not given; f_v was chosen to minimize artifacts in the Kramers-Kronig comparison between $\mathrm{Re}\epsilon_{I2}$ and $\mathrm{Im}\epsilon_{I2}$ over the entire 1.5- to 6.0-eV spectral range. The ratio $(d_2+d_3)/d_1=5.27\pm0.02$ agrees almost exactly with that obtained from Fig. 2, and all other values except d_3 fall within the respective experimental uncertainties. The effective thickness of the microscopically rough region is far too small to be resolved by a transmission-electron microscope; however, it is clear from Fig. 4 that it is present and that its effects cannot be ignored. Figure 4 in effect constitutes an existence proof for this overlayer and justifies the correction of the $\langle\epsilon\rangle$ data above 3 eV for microscopic roughness. The full spectrum for the p-Si layer calculated in this way is given in Fig. 1.

The fact that *all* interference-related artifacts can be eliminated completely by the proper choice of d_1, d_2, d_3, and f_v is extremely significant and has far greater implications than merely achieving the correct values of these parameters. Since any failure of the sample to conform to the basic assumptions of the five-phase model would generate compensating energy-dependent artifacts in ϵ_{I2}, the successful elimination of all such artifacts shows that the films involved are indeed isotropic, uniform, and homogeneous, and that the interfaces are mathematically sharp on the necessary scale. The solution of Eq. (1) is particularly dependent on inhomogeneities near 2.7 eV where the Si film is becoming opaque, owing to a near degeneracy of a number of alternate solutions at that energy. We saw no evidence for any anomalous behavior in this region. This is an independent measure of the uniformity of films and provides further assurance that the calculated dielectric functions are accurate.

We have previously used a five-layer model to nondestructively analyze native oxides on GaAs,[35] where the spectral dependence of the oxide was assumed to have a Sellmeier form. The present approach is more basic in that no *a priori* assumptions are made about the dielectric nature of the overlayer. Only very general (and as discussed above, verifiable) assumptions need be made about the types of layers involved, their homogeneity, and the quality of their interfaces. A difficulty is that a large number of different solutions can be obtained for ϵ_{I2} from Eq. (1). Some of these are shown in Fig. 5. The solutions group into classes according to the order ν of the overall phase shift $2\pi\nu=n_0d_2$, where $n_0=\epsilon^{1/2}$ is the refractive index of the film. For this film, a change in order corresponds to a change in d_2 of about 400 Å. In addition, different solutions for n_0 exist within a given order for different values of d_2. The optimum solutions for $\mathrm{Re}\epsilon_{I2}$ for four orders are shown in Fig. 5 together with a set of solutions for d_2 values differing by 100 Å for the correct order. In this case interference-related structure makes the correct order and solution easy to identify.

IV. RESULTS AND DISCUSSION

As mentioned above, Fig. 1 shows that the effects on ϵ due to a large density of free carriers are relatively small. We discuss the p-Si results according to spectral regions and consider the microstructural and a-Si results at the end.

A. p-Si, region below 2.5 eV

Here, free-carrier effects appear mainly in ϵ_1, causing a reduction of 0.77 at 1.5 eV but becoming essentially unobservable at 2.5 eV. According to the Drude theory we can write

$$\epsilon_p=\epsilon_c-E_p^2/E(E+i\Gamma)\ , \tag{2}$$

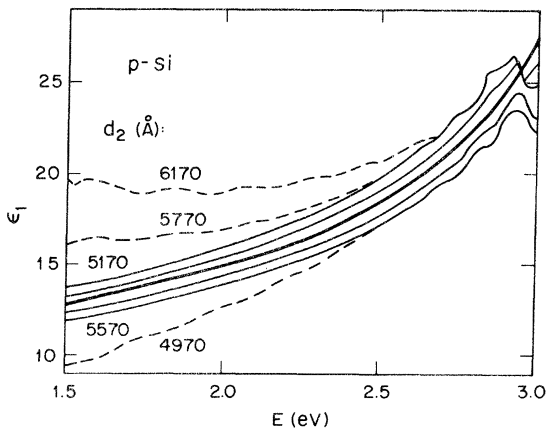

FIG. 5. As Fig. 4, but for the real part of the dielectric function for four different orders $2\pi\nu=n_0d_2$, and for d_2 values in increments of 100 Å for the correct order. Similar sets of solutions exist for the other orders but are not shown.

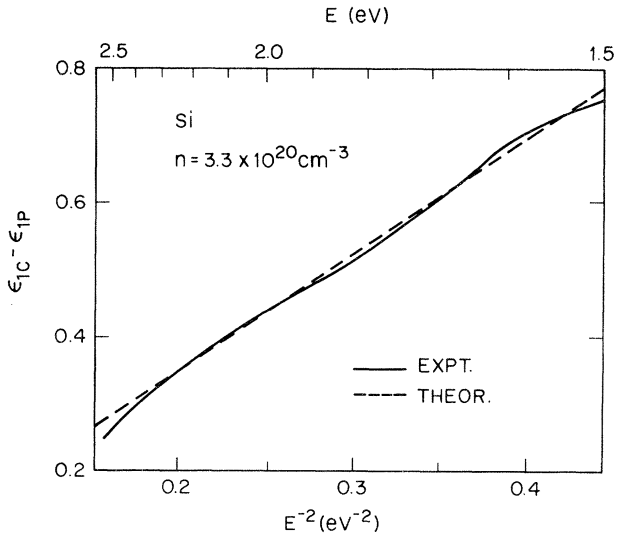

FIG. 6. Difference between ϵ_1 values for lightly doped (ϵ_{1c}) and saturation P-doped (ϵ_{1p}) Si. The theoretical curve passes through the origin and has a slope corresponding to $n=3.3\times10^{20}$ cm^{-3}.

where Γ is the broadening parameter, E_p is the plasma energy, and ϵ_p and ϵ_c are the dielectric functions of p- and c-Si, respectively. Here

$$E_p^2=\frac{4\pi ne^2\hbar^2}{3}\left[\frac{1}{m_l}+\frac{2}{m_t}\right], \tag{3}$$

where for Si $m_l=0.916m_e$ and $m_t=0.191m_e$.[4] For $\Gamma \ll E$, a plot of $(\epsilon_p-\epsilon_c)$ vs E^{-2} should yield a straight line which passes through the origin $1/E^2=0$.

Figure 6 shows that our data plotted in this way agree with the theory to within ±0.02, or to within $\pm0.2\%$ of the local value of $|\epsilon|$, with a slope that corresponds to a free-carrier concentration $n=3.3\times10^{20}$ cm^{-3}. This value can be compared to the known solubility limit of 6×10^{20} cm^{-3} for P in Si at a diffusion temperature of 1000 °C, which results in an electrically active concentration $n=3\times10^{20}$ cm^{-3} of free carriers.[16,17] Thus the effects in this spectral region are entirely due to free carriers with no other factors, such as microstructure, being significant.

The result allows us to draw the following conclusions. First, the polysilicon films prepared as described in the preceding section consist primarily of material that is optically indistinguishable, except for carrier concentration, from lightly doped c-Si. This is entirely reasonable since Fig. 2 shows that the individual grains are large and the grain boundaries can only constitute a small fraction of the volume. Second, the difference $\pm0.2\%$ between theory and experiment establishes the upper limit to the systematic errors in *both* sets of ϵ data, those reported previously[15] for the lightly doped c-Si and those discussed here for heavily doped p-Si. This follows because the former data were obtained in a purely reflection-ellipsometric mode, while the present data are obtained by a combined reflection-transmission approach for which any systematic errors would be quite different.

We can also draw some conclusions about the dominant free-carrier scattering mechanisms from the correspond-

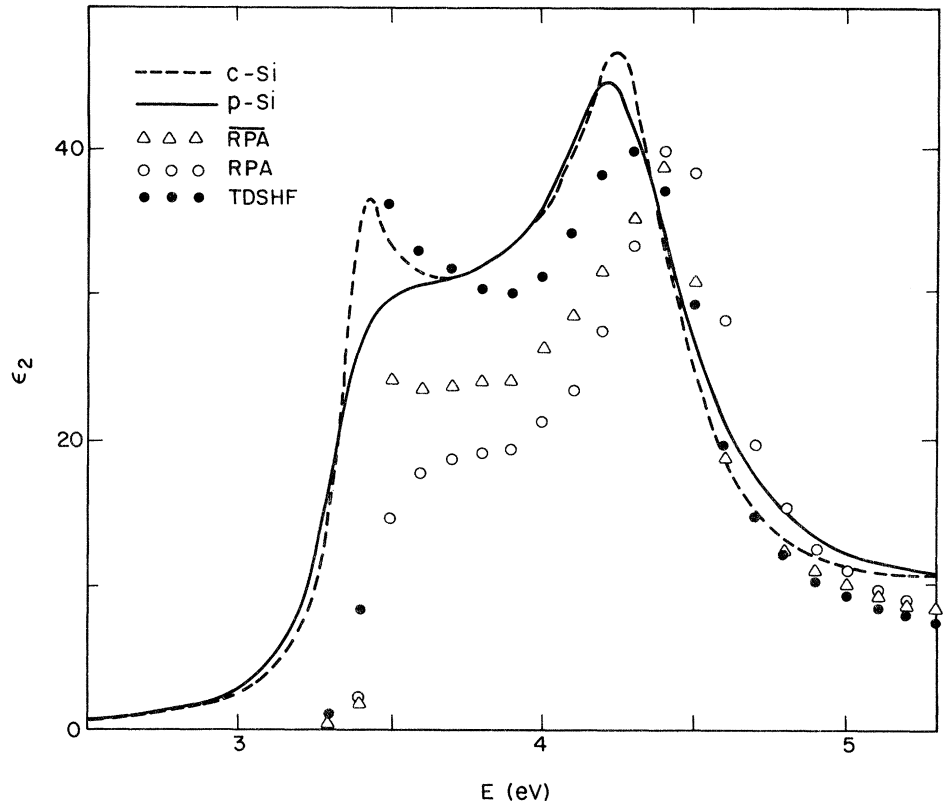

FIG. 7. Calculations of ϵ_2 for Si in the random phase approximation ($\overline{\text{RPA}}$), also including local-field effects (RPA), and also including excitonic effects (TDSHF), from Ref. 18. Data from Fig. 1 are also shown for comparison.

ing difference between the imaginary parts of ϵ, which is not shown but which also decreases approximately as $E^{-2\pm1}$ with a maximum value of 0.08 at 1.5 eV. The functional dependence indicates that the energy loss is primarily due to the interaction of free carriers with lattice vibrations, for which $\Delta\epsilon_2$ should vary as[1] $E^{-2.5}$. The full theoretical expression involves an electron-phonon strength parameter which can be estimated from free-carrier absorption in Ge, for which $\alpha=(2\times10^{17}\ \mathrm{cm}^2)n$ at $\lambda=5\ \mu$m.[2] By scaling the remaining factors to account for the differences between Ge and Si, we calculate $\Delta\epsilon_2=0.08$ at 1.5 eV in agreement with our observations.

Energy loss from charged-impurity scattering should decrease as $E^{-4.5}$, so at sufficiently high energies it should become unimportant with respect to lattice scattering. In this case the theoretical expression[1] can be evaluated from known parameters, and we find that the contribution from charged-impurity scattering should be $\Delta\epsilon_2=0.003$ at 1.5 eV for our sample. This is indeed negligible with respect to lattice scattering. Thus all data below 2.5 eV support the conclusion that the films are completely equivalent to heavily doped but otherwise high-quality single-crystal material.

B. p-Si, region above 2.5 eV

Above 2.5 eV lattice scattering becomes unimportant and the dominant effects are due to the screening of excitonic responses and the shift of the band edges due to electron-electron, electron-ion, and lattice potential effects. We discuss screening effects first.

1. Free carriers and the electron-hole interaction

The effect of the electron-hole interaction on higher-interband optical spectra has recently been discussed in detail by Mattausch, Hanke, and Strinati (MHS),[18] who began with a one-electron random-phase approximation (RPA in their notation), added local-field effects (RPA), and finally considered both local-field and electron-hole interactions in a time-dependent screened Hartree-Fock approximation (TDSHF). The results of their calculations are compared to our spectra in Fig. 7. It should be remembered that their results strictly apply only to undoped material, and for this case the agreement between the computed TDSHF and measured c-Si spectra is reasonably good. The upward energy shift of all structures in their calculated spectra is probably due in part to their use of the results of early reflectance data[36] in establishing the parameters used in their calculation. As MHS emphasize, both local-field and electron-hole interactions are needed to obtain the necessary amplitude to ϵ_2 in the E_1 region. MHS attribute the lower calculated amplitude of E_2 to details of the relatively complicated band structure giving rise to this spectral feature. As mentioned above, the most striking aspect of the ϵ_2 spectrum of the heavily doped sample is its overall similarity to that of the highly doped single crystal. We can therefore conclude on the basis of the MHS calculations that carrier densities $\sim3\times10^{20}\ \mathrm{cm}^{-3}$ are not sufficient to significantly perturb either local-field or electron-hole interactions with respect to general states in the zone. If the electron-hole interaction were markedly reduced, the ϵ_2 spectrum would tend toward the RPA curve, and Fig. 7 shows that this is not the case.

The major difference between the two experimental spectra is the loss of the peak structure near E_1 in that for the heavily doped material. This effect has also been reported for ion-implanted and laser-annealed Si.[37] Since the E_1 structure is generally considered to originate in part from a metastable bound exciton in the lightly doped material,[37] its loss at large carrier densities is not surprising. This conclusion can be supported quantitatively: The Thomas-Fermi screening length L_{TF} for Si can be represented by[4]

$$L_{\mathrm{LF}}^2=\frac{\hbar^2\epsilon_0}{4um^*e^2}\left[\frac{\pi u}{3n}\right]^{1/3}, \tag{4}$$

where $\epsilon_0=11.4$ is the static dielectric constant, $m^*=(m_l m_t^2)^{1/3}=0.32m_e$ is the density-of-states effective mass, and $u=6$ is the number of equivalent conduction-band minima. From these results we calculate $L_{\mathrm{TF}}=5$ Å.

If the exciton radius for a given critical point is larger than L_{TF}, then the sharp excitonic structure for that critical point should be absent.[38] Interband reduced masses in the range of $0.022-0.11m_e$ have been reported for the E_1 and $E_1+\Delta_1$ transitions in Si; the former was derived from electroreflectance measurements[39] and concerns primarily the spin-orbit-split valence band, which is severely distorted in Si by the k-linear interaction.[40] The latter was obtained from a combined electroreflectance-ellipsometric study,[41] and is more appropriate for the present measurements where a large density of states is more important than a small effective mass. Using the larger value, which is actually more conservative in this calculation, and supposing that the mass is sufficiently large along $\langle 111\rangle$ so that the critical point can be considered two dimensional, we calculate an excitonic radius of 28 Å. Thus the peak in ϵ_2 at E_1 should be eliminated if it is excitonic in origin, as observed.

A similar calculation can be performed for the E_2 peak using the effective-mass approximation to estimate the mass involved. The calculation shows that any E_2 exciton should be similarly screened at these carrier densities. The fact that no significant change occurs at E_2 indicates that no significant excitonic resonance is developed at the Brillouin-zone regions involved.

2. Energy threshold effects

As recently discussed by Berggren and Sernelius,[4] Selloni and Pantelides,[5] and Allen and co-workers[20–22] heavy doping can affect threshold energies by a number of independent mechanisms. Electron-electron and certain screened electron-ion contributions to the electron and hole self-energy terms have been evaluated by Berggren and Sernelius[4] for the fundamental indirect gap of Si. They find that exchange and correlation effects produce a shift proportional to $n^{1/3}$, a consequence of a dependence on the Fermi momentum k_F, while screened electron-ion interactions provide a $n^{1/2}$ dependence. Allen and co-workers[20–22] have predicted a linear dependence on n re-

sulting from ensemble averages over form and structure factors for impurity atoms distributed at random sites over the lattice. General expressions are given in each case, but they are complicated. Moreover, the quantitative results depend rather strongly on various assumptions. For example, Selloni and Pantelides[5] showed a strong contribution from intervalley scattering terms neglected by previous workers. Evaluation of these expressions is beyond the scope of the present paper; instead, we restrict our attention to possible functional dependences of the E_1 and E_2 thresholds on n.

Figure 8 summarizes the results of our present work, our previous results on As-implanted and laser-annealed Si crystals,[7] and recent spectroscopic ellipsometric results by Viña and Cardona[19] for both E_1 and E_2 transitions. We had previously concluded[7] on the basis of numerical differentiation and line-shape fitting that both thresholds varied approximately linearly in n, while Viña and Cardona concluded[19] that their data could not discriminate between a $n^{1/3}$ and n (and presumably $n^{1/2}$) dependence. Since linear filtering algorithms can introduce systematic shifts under combined differentiation-smoothing operations, we reevaluated our threshold energies using more accurate Fourier methods of critical-point analysis recently developed by us.[42,43] This approach takes advantage of the phase-coherent property of a singularity in reciprocal space, which allows threshold energies to be determined from the rate of change of the phases of successive Fourier coefficients with coefficient index. Neither numerical differentiation, digital smoothing, nor base-line information are required, so accuracy is improved by eliminating certain classes of systematic errors. Moreover, the assumption of a single-critical-point representation can be assessed directly.

As an example, we show in Fig. 9 the phases of the Fourier coefficients of the segments of the spectra of Fig. 1 in the vicinity of the E_2 transitions as a function of index for a zero-phase energy reference of 4.25 eV. Theoretical trajectories in 10-meV increments for ideal critical points show that a single critical-point representation is valid to within about ± 4 and ± 10 meV for the undoped c-Si and saturation P-doped p-Si samples, respectively. The relevant E_2 threshold energies are 4.29 and 4.21 eV. A similar analysis was performed to obtain the threshold energies of the E_1 critical points. In addition, we reanalyzed our stored data reported in Ref. 7 by this method. Consequently, a comparison of threshold energies from these sources is valid since they were all calculated in the same way. On the other hand, Viña and Cardona analyzed their spectra by real-space numerical differentiation-smoothing algorithms, which unnecessarily attenuate the high-index Fourier coefficients and can produce unintended systematic errors in computed threshold energies.[42] For example, we find from our data for undoped samples that the E_1 critical point energy is 10 meV lower if calculated by real-space analysis followed by curve fitting, in agreement with the discrepancy seen in Fig. 8.

The Fourier-derived threshold energies do not provide enough data to definitively assign a functional dependence, but suggest rather strongly a linear dependence for E_1 and are consistent with a linear dependence for E_2.

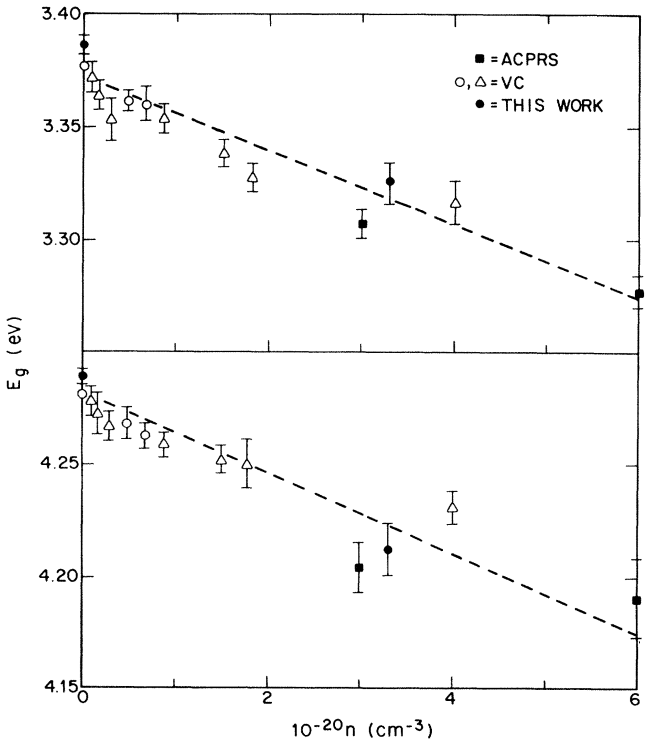

FIG. 8. Dependence of threshold energies of the E_1 and E_2 critical points on carrier concentration n. Solid circles, present work; solid squares, Ref. 7; open circles, n-type material, from Ref. 19; open triangles, p-type material, from Ref. 19.

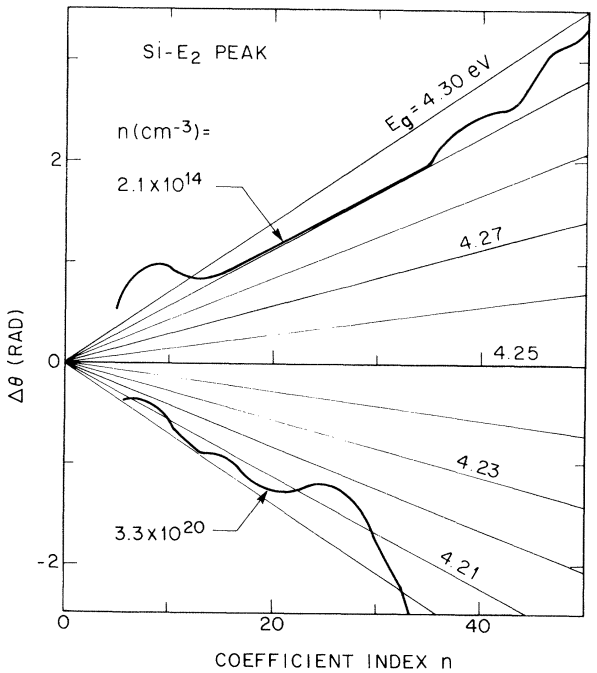

FIG. 9. Phase vs coefficient index plots for determining the threshold energy and validity of a single-critical-point representation for the E_2 transition of Si samples with carrier concentrations as indicated.

These data, which cover a somewhat larger range of impurity concentrations than those given in Ref. 19, do not show the tendency toward saturation exhibited by the data of Ref. 19. Only the data reported in the present work were obtained on samples where the free-carrier density was measured directly. The data in Ref. 7 were obtained on samples for which the total As-impurity concentration was measured independently by Rutherford backscattering. The agreement in threshold energies between the present data and the comparably doped samples of Ref. 7 indicate that essentially all the As impurities in these laser-annealed samples were electrically active. The method of determining free-carrier concentration in Ref. 19 was not specified; if the electrically active impurity concentration became progressively less than the total impurity concentration with increasing concentration, then the tendency toward saturation in the Ref. 19 data would be readily explained.

Despite these differences, Fig. 8 shows that all threshold data are generally consistent with a linear slope of approximately 0.02 eV/10^{20} cm^{-3} for both E_1 and E_2 structures. The curvature present below 10^{20} cm^{-3} in the Ref. 19 data occurs in a range where a $n^{1/3}$ or $n^{1/2}$ dependence would be expected to be dominant. However, the magnitudes of these possible $n^{1/3}$ or $n^{1/2}$ contributions are far less than those predicted by many-body calculations for the fundamental indirect gap and also less than those predicted for the top of the valence band separately. Berggren and Sernelius show that electron-electron ($n^{1/3}$) and screened electron-ion ($\sim n^{1/2}$) effects should raise the top of the valence band by $\sim$40 and $\sim$20 meV, respectively, at $n=10^{20}$ cm^{-3}. But these effects are k dependent and since neither E_1 nor E_2 involve zone-center states the results may not be directly applicable. Further calculations would be necessary to resolve this point. The present results indicate that self-energy effects for these critical points should be much less than the effects at the fundamental indirect gap.

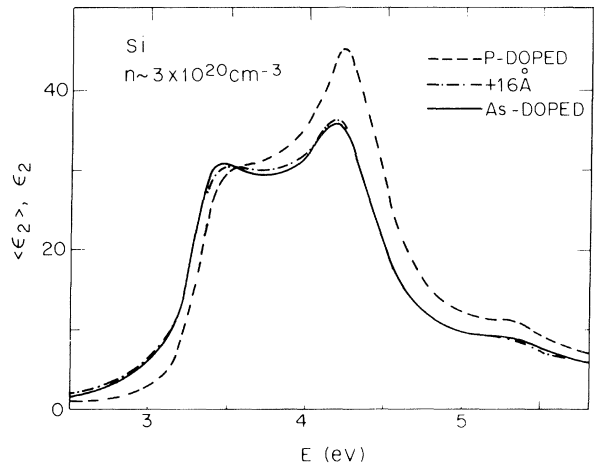

FIG. 10. Solid curve: imaginary part of the pseudodielectric function of an As-implanted laser-annealed Si wafer with $n=3\times10^{20}$ cm^{-3}, from Ref. 7. Dashed curve: ϵ_2 spectrum for p-Si with $n=3.3\times10^{20}$ cm^{-3}, from Fig. 1. Dot-dashed curve: $\langle\epsilon_2\rangle$ curve calculated by assuming a 16-Å microscopically rough layer with 50- vol % voids on the surface of the p-Si sample.

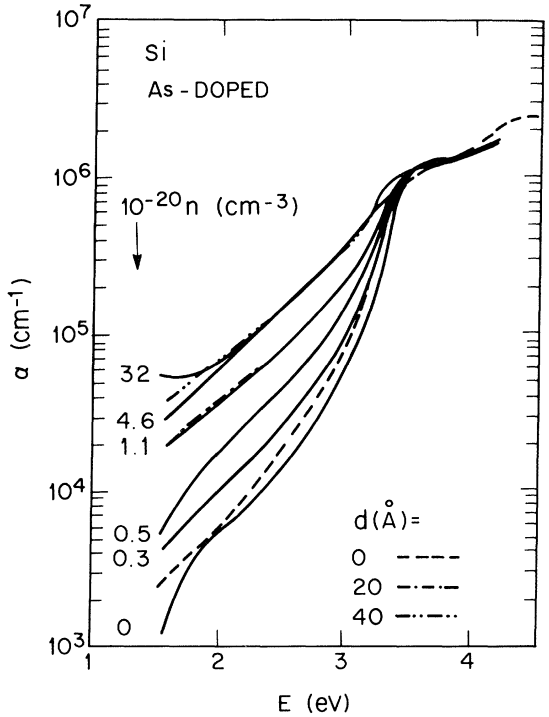

FIG. 11. Solid curves: absorption-coefficient data for lightly doped c-Si and As-implanted laser-annealed c-Si for impurity concentrations as indicated, from Ref. 8. Dashed curve: ϵ_2 data for p-Si with $n=3.3\times10^{20}$ cm^{-3}, from Fig. 1. Dot-dashed curves: Pseudoabsorption-coefficient spectra calculated by assuming 20- and 40-Å microscopically rough layers with 50-vol % voids on the surface of the p-Si sample.

A linear shift can be attributed to changes in the average or effective pseudopotentials of the Si-P or Si-As lattice due to the presence of substitutional donors on the lattice sites. The general formalism has been given by Allen and co-workers.[20–22] The dominant effect would be expected to arise from an ensemble average over randomly placed donors via a second-order coupling to intermediate states. The first-order term is weak and, in any case, would predict a difference between n- and p-type samples that is not seen experimentally.[19]

C. p-Si, microstructural effects

Having obtained accurate ϵ data for heavily doped Si, we can now examine previous data for the existence of microstructural effects. By so doing, we resolve some remaining questions about the apparent physics of heavy doping, in particular, the differences among laser-annealed samples with As or P as recently reported by Jellison and co-workers.[8]

We consider first our earlier results[7] on As-implanted laser-annealed c-Si wafers. Figure 10 shows a comparison between measured $\langle\epsilon\rangle$ spectra for a laser-annealed sample implanted with 3×10^{20} cm^{-3} As and the p-Si data of Fig. 1 determined from a P-doped sample with the same impurity concentration. The amplitudes of the E_2 peaks differ by 25% and the E_1 edge of the laser-annealed sample is apparently downshifted by 10 meV, indicating at first sight a substantial difference between As and P dop-

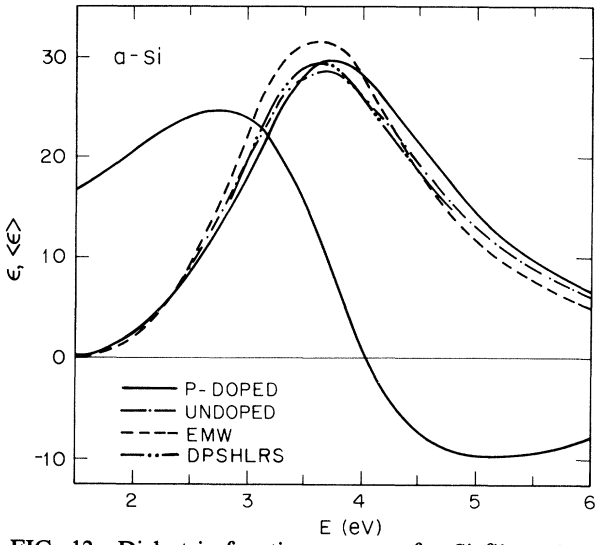

FIG. 12. Dielectric function spectra of a-Si films obtained from different sources. Solid curve: *in situ* P-doped LPCVD film, this work. Dot-dashed curve: undoped LPCVD film, from Ref. 23. Dashed curve: glow-discharge film, from Ref. 44. Double-dotted—dashed curve: multipole-plasma film, from Ref. 24.

ing. But if we calculate an $\langle\epsilon\rangle$ spectrum assuming the p-Si sample is covered with a microscopically rough surface region 16 Å thick and described by an EMA mixture containing 50 vol% voids, we find that the calculated spectrum is virtually identical to that of the laser-annealed sample as also shown in Fig. 10. Thus the apparently large differences between As and P dopants, at least to an impurity concentration of 3×10^{20} cm^{-3}, can be entirely understood in terms of microstructure.

With this background, we now investigate the differences in optical spectra between As- and P-implanted laser-annealed material in the recently reported SE measurements of Jellison and co-workers.[8] Their results, expressed as an absorption coefficient α, are reproduced in Fig. 11 together with the α spectrum calculated from the p-Si data of Fig. 1. The p-Si α spectrum is in good agreement with that for the lightly doped c-Si sample from Ref. 8, which in turn was also very similar to that observed in Ref. 8 for P-implanted and laser-annealed material. In contrast, the absorption coefficient data for the As-implanted and laser-annealed samples show a monotonic increase with As concentration, suggesting a fundamental difference in the materials. But if we again calculate pseudoabsorption-coefficient spectra assuming microscopically rough surface regions 20 and 40 Å thick, we reproduce almost exactly the data for the As-doped samples with $n=1.1\times10^{20}$ cm^{-3} and 3.2×10^{21} cm^{-3}, respectively. In fact, the agreement in the former case is so good that the difference cannot be seen clearly on this scale. Thus, as with Fig. 10, we can conclude that the apparently larger absorption coefficients have nothing to do with an intrinsic difference between As and P as dopants but are entirely due to microstructural differences that occur on recrystallization. The same conclusion follows from a detailed analysis of the pseudorefractive-index data of Fig. 1 in Ref. 8.

While the results show that As and P *as dopants* are essentially interchangeable, it is nonetheless clear that the *microstructural* differences caused by As and P implantation are nevertheless quite real. The difference is probably due to differences in rates of recrystallization or ease of regrowth of laser-annealed Si samples implanted with P or As.

D. Amorphous material

Similar analyses were performed on a-Si films doped *in situ* with phosphorus and deposited via LPCVD at 571 °C. The ϵ spectrum for such a film is shown in Fig. 12. The ellipsometric data were analyzed by the methods of Sec. II, and the microstructural parameters in this case were found to be $d_1=990\pm25$ Å, $d_2=5487\pm10$ Å, and $d_3=19.5\pm0.5$ Å. The values of d_1 and d_2 are in good agreement with those expected from the processing history of the sample. The best results were obtained for the microscopically rough surface having 50 vol% voids. The surface layer thickness was somewhat larger than that of the p-Si film discussed in the preceding section.

The spectrum in Fig. 12 shows typical amorphous character with ϵ_2 rising smoothly to a peak of 29.6 at 3.74 eV. For comparison, similar data on a number of undoped a-Si films are also shown. The spectrum of Ewald *et al.*[44] was obtained from reflectance data taken on a glow-discharge-deposited sample prepared with a substrate temperature of 400 °C. To obtain the ϵ_2 spectrum, the reflectance data were extrapolated beyond the experimentally accessible energy range of 1.5—10.0 eV and Kramers-Kronig transformed.[44] The spectrum of Drevillon *et al.*[24] is actually a $\langle\epsilon\rangle$ spectrum calculated without regard to overlayer corrections from spectroscopic ellipsometric data for a a-Si film deposited at 340 °C from a low-

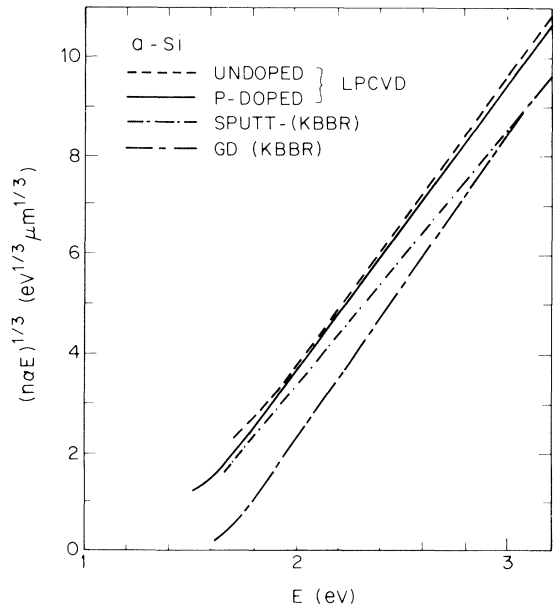

FIG. 13. Variation of $(\alpha nE)^{1/3}$ vs energy of the LPCVD samples of Fig. 12, together with data of sputtered- and glow-discharged films from Ref. 28.

pressure multipole plasma. This film had an estimated density of 97±4% as determined from combined Rutherford backscattering areal density and spectroscopic ellipsometric thickness measurements, and a hydrogen content of the order of 5%. Data that we previously reported[23] for an undoped LPCVD film deposited at 625 °C are also shown after correction for a 4 Å overlayer of microscopic roughness. This thickness was determined by an analysis of interference oscillations similar to that shown in Fig. 4, but the oscillations could not be made to vanish in this case so the thickness results are not conclusive. Quite possibly considerable recrystallization had already occurred in the lower regions of that film at that deposition temperature,[13] so the inability of a simple model to describe this film is not surprising.

Nevertheless, all spectra in Fig. 12 are remarkably similar, suggesting that a general convergence of various groups to the "intrinsic" dielectric properties of dense a-Si has now occurred. The data of Ewald *et al.*[44] are not expected to be as accurate owing to artifacts peculiar to the Kramers-Kronig analysis. The data of Drevillon *et al.*[24] may show small distortions since no correction was made for surface roughness. The difference between our present data for heavily doped a-Si and our previous data for the undoped film vanishes completely if we assume that the thickness of the microscopically rough layer on the latter sample was 9.6 Å instead of 4.0 Å. Thus the differences among ϵ_2 spectra of all samples can be attributed to microstructure, and we conclude that no effect unambiguously related to the large density of free carriers is present.

Because our present data accurately cover a dynamic range of α of nearly 1000, we can also accurately investigate various theoretical predictions for functional dependences of optical parameters on energy as a means of understanding in more detail the electronic energy levels and absorptive processes in a-Si. Tauc *et al.*[25] originally proposed a linear variation of $(E^2\epsilon_2)^{1/2}$ with E, which follows for constant-momentum matrix elements in a simple nondirect transition model between parabolic bands, while Davis and Mott[26] proposed a linear variation of $(\alpha nE)^{1/3}$ as a means of unifying both Urbach-edge broadening and frozen-in structural disorder by taking the momentum matrix element to vary linearly in energy. More recently, Cody *et al.*[27] proposed that a linear variation of $(\epsilon_2)^{1/2}$ vs E would be an indication of a constant-dipole matrix element for nondirect transitions between simple parabolic bands.

In agreement with Klazes *et al*,[28] we found much better agreement with the Davis-Mott functional form and with that proposed by Cody *et al.* than with the Tauc expression. Our results for both heavily P-doped and undoped LPCVD samples are shown in Fig. 13 as $(\alpha nE)^{1/3}$ together with selected results from Ref. 28. The very nearly equivalent slopes and extrapolation energies for the two LPCVD samples provide further evidence that the incorporation of large numbers of dopant atoms has very little effect on the properties of a-Si. In addition, these plots are very sensitive to microscopic roughness. The fact that straight lines are obtained for the LPCVD samples is another indication that microscopic roughness has been accounted for successfully. The extrapolated energy of 1.4 eV is close to that for the sputtered-sample data of Ref. 28, although the slope of the latter is somewhat reduced suggestive of a lower density in this material. The slope of the data for the glow-discharge sample is in agreement with that obtained for the LPCVD material; since the glow-discharge sample was deposited at 370 °C and can therefore be expected to be relatively free of hydrogen, the difference in extrapolated zero crossings probably indicates a lower density of intrinsic states. The relatively large α values of the LPCVD material prevented a meaningful comparison to the earlier theory of Cody *et al.*,[45] which predicts a Urbach-type edge due to frozen-in disorder.

We have not shown our data expressed as $(\epsilon_2)^{1/2}$ because the difference in linearity is too small to be meaningful. In fact, both forms $(\alpha nE)^{1/3}$ and $(\epsilon_2)^{1/2}$ are very closely related in that if $(\epsilon_2)^{1/2}$ varies linearly in energy, then $(\alpha nE)^{1/3}$ will vary as $E^{4/3}$. This difference is difficult to detect over a relatively narrow range in energy. While our data can eliminate the simple model of Tauc *et al.*,[25] they cannot distinguish between the models proposed by Davis and Mott[26] and by Cody *et al.*[27]

ACKNOWLEDGMENTS

It is a pleasure to express our thanks to M. Sternheim for preparing the LPCVD samples and to R. Knoell for obtaining the TEM micrograph.

*Present affiliation: Central Services Organization of the Bell Operating Companies.

[1]H. Y. Fan, W. Spitzer, and R. J. Collins, Phys. Rev. 101, 566 (1956).

[2]H. Y. Fan, in *Semiconductors and Semimetals,* edited by R. K. Willardson and A. C. Beer (Academic, New York, 1967), Vol. 3, p. 405.

[3]R. W. Keyes, Comments Solid State Phys. 7, 149 (1977).

[4]K.-F. Berggren and B. E. Sernelius, Phys. Rev. B 24, 1971 (1981).

[5]A. Selloni and S. T. Pantelides, Physics 117&118B, 78 (1983).

[6]M. Cardona and H. S. Sommers, Jr., Phys. Rev. 122, 1382 (1961).

[7]D. E. Aspnes, G. K. Celler, J. M. Poate, G. A. Rozgonyi, and T. T. Sheng, in *Laser and Electron Beam Processing of Electronic Materials,* edited by C. L. Anderson, G. K. Celler, and G. A. Rozgonyi (Electrochemical Society, Princeton, 1980), Vol. 80-1, p. 414.

[8]G. E. Jellison, Jr., F. A. Modine, C. W. White, R. F. Wood, and R. T. Young, Phys. Rev. Lett. 46, 1414 (1981).

[9]D. E. Aspnes, Thin Solid Films 89, 249 (1982).

[10]D. E. Aspnes, Physica 117&118B, 359 (1983).

[11]A. C. Adams, D. E. Aspnes, and B. G. Bagley, U. S. Pat. No. 4357179, issued 2 Nov. 1982.

[12]E. Kinsbron, M. Sternheim, T. T. Sheng, and S. Vaidya, Electronic Materials Conference, Fort Collins, Colorado, 1982 (unpublished).

[13]E. Kinsbron, M. Sternheim, and R. Knoell, Appl. Phys. Lett. 42, 835 (1983).
[14]A. Bauderant and M. Sacilotti, J. Electrochem. Soc. 129, 1119 (1982).
[15]D. E. Aspnes and A. A. Studna, Phys. Rev. B 27, 985 (1983).
[16]R. B. Fair and J. C. C. Tsai, J. Electrochem. Soc. 124, 1107 (1977).
[17]N. Lifshitz, J. Electrochem. Soc. 130, 2464 (1983).
[18]H. J. Mattausch, W. Hanke, and G. Strinati, Phys. Rev. B 27, 3735 (1983).
[19]L. Viña and M. Cardona, Physica 117&118B, 356 (1983).
[20]P. B. Allen and V. Heine, J. Phys. C 9, 2305 (1976).
[21]P. B. Allen, Phys. Rev. B 18, 5217 (1978).
[22]B. Chakraborty and P. B. Allen, Phys. Rev. B 18, 5225 (1978).
[23]B. G. Bagley, D. E. Aspnes, A. C. Adams, and F. B. Alexander, Jr., Bull. Am. Phys. Soc. 25, 12 (1980).
[24]B. Drevillon, J. Perrin, J. M. Siefert, J. Huc, A. Lloret, G. de Rosny, and J. P. M. Schmitt, Appl. Phys. Lett. 42, 801 (1983).
[25]J. Tauc, R. Grigorovici, and A. Vancu, Phys. Status Solidi 15, 627 (1966).
[26]E. A. Davis and N. F. Mott, Philos. Mag. 22, 903 (1970).
[27]G. D. Cody, B. G. Brooks, and B. Abeles, Solar Energy Mater. 8, 231 (1982).
[28]R. H. Klazes, M. H. L. M. van den Broek, J. Bezemer, and S. Radelaar, Philos. Mag. B 45, 377 (1982).
[29]D. E. Aspnes and A. A. Studna, Appl. Phys. Lett. 39, 316 (1981).
[30]D. E. Aspnes and A. A. Studna, Appl. Opt. 14, 220 (1975); *Society of Photo-Optical Instrumention Engineers Proceedings* 112, 62 (1977); Rev. Sci. Instrum. 49, 291 (1978).
[31]D. E. Aspnes, J. Opt. Soc. Am. 64, 812 (1975); D. M. Radman and B. D. Cahan, *ibid.* 71, 1546 (1981).
[32]I. H. Malitson, J. Opt. Soc. Am. 55, 1205 (1965).
[33]See, e.g., R. M. A. Azzam and N. M. Bashara, *Ellipsometry and Polarized Light* (North-Holland, Amsterdam, 1977).
[34]D. A. G. Bruggeman, Ann. Phys. (Leipzig) 24, 636 (1935).
[35]D. E. Aspnes, G. P. Schwartz, G. J. Gualtieri, A. A. Studna, and B. Schwartz, J. Electrochem. Soc. 128, 590 (1981).
[36]H. R. Philipp, J. Appl. Phys. 43, 2835 (1972).
[37]G.-J. Jan, F. H. Pollak, and R. Tsu, Solar Energy Mater. 8, 241 (1982).
[38]J. Gay, Phys. Rev. B 4, 2567 (1971).
[39]J. Grover and P. Handler, Phys. Rev. B 9, 2600 (1974).
[40]M. Cardona, Phys. Rev. B 15, 5999 (1977).
[41]A. Daunois and D. E. Aspnes, Phys. Rev. B 18, 1824 (1978).
[42]D. E. Aspnes, Surf. Sci. 135, 284 (1983).
[43]D. E. Aspnes and H. Arwin, J. Opt. Soc. Am. 73, 1759 (1983).
[44]D. Ewald, M. Milleville, and G. Weiser, Philos. Mag. B 40, 291 (1979).
[45]G. D. Cody, T. Tiedje, B. Abeles, B. Brooks, and Y. Goldstein, Phys. Rev. Lett. 47, 1480 (1981).

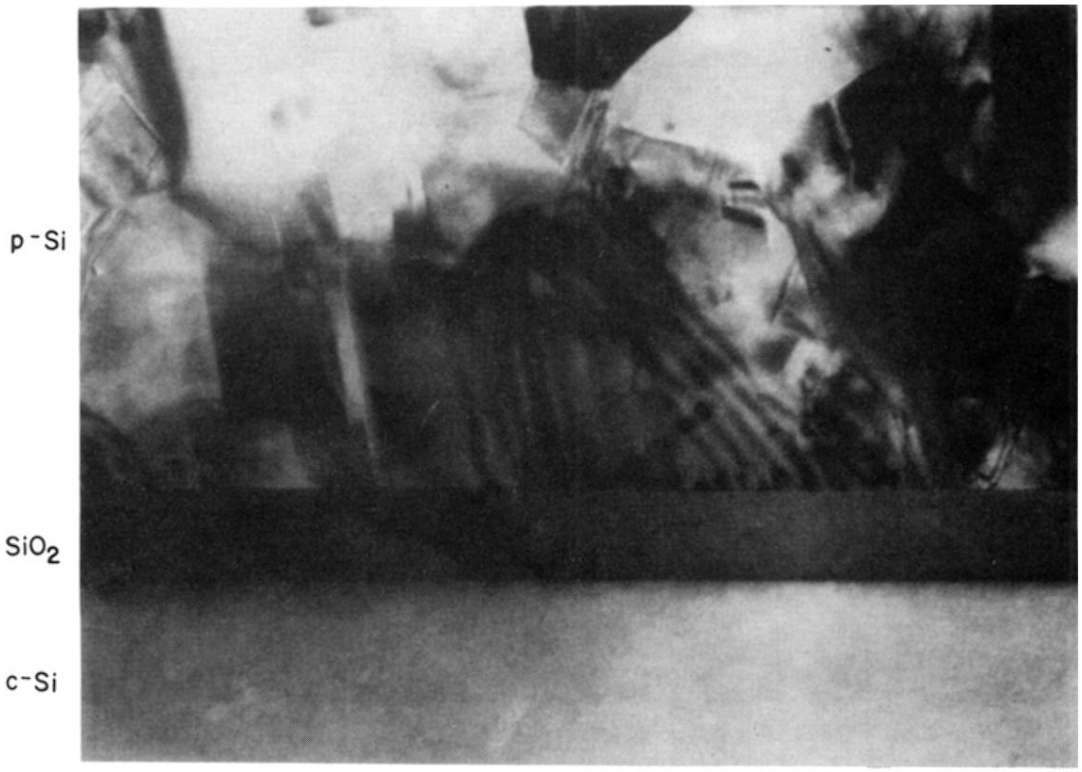

FIG. 2. Micrograph of the cross section of the heavily doped large-grain polycrystalline film used to obtain the data of Fig. 1. The 1000-Å thermal oxide and single-crystal Si substrate are the dark and light gray regions, respectively.